JOURNAL OF SOLID STATE CHEMISTRY **128,** 220–227 (1997)
ARTICLE NO. SC967191

The Syntheses and Structures of the Complex Oxide Carbonates $Ba_{11}Pd_{11}O_{20}(CO_3)_2$ and $Ba_{88}Ni_{87}O_{156}(CO_3)_{19}$

R. J. Crooks and M. T. Weller[1]

Department of Chemistry, University of Southampton, Highfield, Southampton SO17 1BJ, United Kingdom

Received June 20, 1996; in revised form October 9, 1996; accepted October 15, 1996

A new palladate analog, $Ba_{11}Pd_{11}O_{20}(CO_3)_2$, of the complex copper oxide carbonate, $Ba_{44}Cu_{48}(CO_3)_6O_{87.9}$, has been synthesized by reaction of PdO and $BaCO_3$ at 810°C. The structure of this phase and the isostructural nickelate have been refined from high resolution powder neutron diffraction data. The structure consists of cages $M_{18}O_{24}$ and M_6O_{12} rings (M = Pd, Ni) separated by barium ions and carbonate groups. A section of the structure separating two $M_{18}O_{24}$ units is strongly disordered and has been refined as containing either carbonate groups or isolated MO_4 square planes. The presence and symmetry of the carbonate groups in these structures has been investigated by infrared and Raman spectroscopy.

INTRODUCTION

The study of complex copper oxides has gained impetus from the discovery of high temperature superconductivity in these materials. Important new areas of solid state chemistry which have emerged as a result of this work include the characterization of Aurivillius type phases with Tl_2O_2 layers (1), complex oxide fluorides (2), and perovskite based structures containing anions such as CO_3^{2-} (3), NO_3^{2-} (3), BO_3^{3-} (4), PO_4^{3-} (5), and SO_4^{2-} (5). The discovery that solid state preparations at high temperatures could incorporate these ions is not new; for example, carbonate containing structures prepared at high temperatures have been described previously (6, 7). One important phase which has recently been found to contain the carbonate ion is barium cuprate, "$BaCuO_2$," a phase that is parasitic in the synthesis of many superconducting materials (8). The structure has been studied by a number of workers, but was initially determined by Kipka and Müller-Buschbaum (9) from a single crystal study. Later refinements (10) build upon this model with slight modifications in terms of the occupation of a barium site and the distribution of copper and oxygen. More recently the structure was refined by Aranda and Attfield using a combined analysis of powder X-ray and powder neutron diffraction data and was shown to contain carbonate ions yielding a true compound stoichiometry of $Ba_{44}Cu_{48}(CO_3)_6O_{87.9}$ (11). The carbonate ions were found to stabilize the structure occupying positions between two Cu_6O_{12} rings. However, there are still some unusual features of the refinement including a Cu–O distance of 1.69 Å. The structure of barium cuprate has been investigated again more recently by Guskos *et al.* (12) though the use of powder X-ray data alone and the introduction of many constraints in the refinement throws doubt on the validity of the positions determined.

The structural chemistry of copper 2 + contains many examples of square planar coordination with Cu–O distances of approximately 1.96 Å typical of Cu^{2+}. Compounds including this unit include Sr_2CuO_3 (13) and superconductors such as $Tl_2Ba_2Ca_3Cu_4O_{12}$ (14) and Bi_2CuO_4 (15). Square planar MO_4 units containing M^{2+} are also a feature of palladium and, to a lesser degree, nickel chemistry and this leads to the formation of a number of structural analogs between palladium/nickel chemistry and copper chemistry. For example, Sr_2PdO_3 (16) and Bi_2PdO_4 (17) have the same structures as the corresponding cuprates. While direct structural analogs for purely square-planar copper and nickel are not known, for higher coordination numbers, e.g., square pyramidal and distorted octahedral, there are many similar structures, e.g., La_2MO_4 (18, 19) $TlSr_2MO_5$ (20, 21). A nickel analog of barium cuprate was reported by Gottschall *et al.* (22); while the stoichiometry determined for this compound is slightly different, the structure is similar with nickel oxide cages and rings. However, the structural work reported in this article was based on a simulated fit to the experimental X-ray pattern confirming only the similarity in structural features.

In this article we report the synthesis of a palladate analog of barium copper oxide carbonate and its structure refinement using high resolution powder neutron diffraction data. The structure of the previously reported barium nickel oxide carbonate is also refined using this technique.

[1] To whom correspondence should be addressed.

0022-4596/97 $25.00

EXPERIMENTAL

Synthesis

"$BaPdO_2$" was synthesized by the direct solid state reaction of intimately mixed $BaCO_3$ (99.95%) and $PdO \cdot xH_2O$ (99.9%) (x determined by TGA as ~ 0.2) at 810°C in air for 24 h. The sample, with a 1:1 molar ratio of barium to palladium, was repeatedly reground and refired until powder X-ray diffraction indicated a monophasic product.

"$BaNiO_2$" was prepared in accordance with Gottschall and Schöllhorn (22). An intimate mixture of $BaCO_3$ (99.95%) and green NiO (99.99%), again a 1:1 molar ratio, was fired at 1025°C under flowing nitrogen, for a total of 32 h, with three intermediate regrinds.

Characterization

Powder X-ray diffraction data were collected over the 2θ range from 14.5° to 114.5° on a Siemens D5000 diffractometer ($\lambda = 1.5406$ Å) on both samples. Initial analysis of the data from the palladate showed it to exhibit features similar to those of barium copper oxide. The cell parameter, later refined using the GSAS profile refinement suite, was initially determined as approximately 18.4 Å, slightly larger than the cuprate, and a very low level of palladium metal could also be discerned in the powder profile. Powder diffraction data from the barium nickelate were in agreement with those published by Gottschall (22) for cubic barium nickel oxide with some weak reflections from residual NiO.

Powder neutron diffraction data were obtained at 298 K, using HRPD, the high resolution powder diffractometer on ISIS at the Rutherford Appleton Laboratory. Each sample was sealed into a thin wall vanadium can and the data were collected using the backscattering detectors with the sample in the 1 m position over a period of 14 h. Preliminary analysis involved focusing the data from the various detectors and correction for the incident beam profile.

The presence of carbonate within the structure of $BaPdO_2$ has been confirmed using infrared spectroscopy (PE Paragon 1000 FT-IR) (Fig. 1). Table 1 details the bands seen in the spectrum and their assignments. The presence of the symmetric stretch, ν_1, in the infrared spectrum, together with a loss of degeneracy of both the ν_3 and ν_4 stretches, suggests the lowering of the local symmetry of the carbonate group from D_{3h} (discrete planar CO_3) to at least C_{2v}. This is consistent with a distortion to C_{2v} indicated from the refined atomic positions which yielded two different C–O bond lengths, *vide infra*. Peaks characteristic of carbonate have also been identified for $BaNiO_2$. The high absorbance of this black compound has led to increased noise in the spectrum, however the presence of the ν_1 vibration indicates a similar local symmetry to the $BaPdO_2$ case. Table 2 shows the infrared band assignments.

Attempts to obtain Raman spectra from both compounds were undertaken using a Perkin–Elmer system 2000 FT Raman spectrometer operating with a Nd-YAG laser. However, problems with sample absorption and fluorescence resulted in poor quality spectra though the presence of

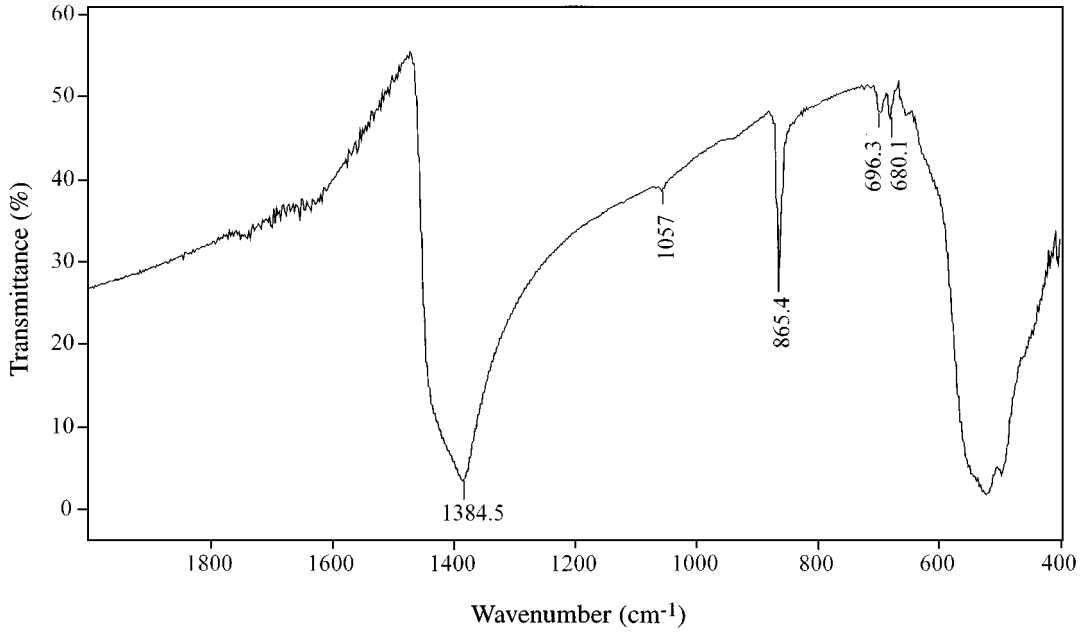

FIG. 1. Infrared spectrum of $BaPdO_2$ in the range 400–2000 cm^{-1} as a KBr disk.

TABLE 1
Vibrational Spectroscopy Data and Assignment of $BaPdO_2$

Infrared wavelength/cm^{-1}	Raman wavelength/cm^{-1}	Vibrational assignment in C_{2v} symmetry
1420–1360	—	$\nu_3(A_1 + B_1)$
1057.1	1061	$\nu_1(A_1)$
865.4	—	$\nu_2(B_1)$
696.3, 680.1	699/—	$\nu_4(A_1 + B_2)$

carbonate in the palladate was confirmed with the observation of the ν_1 mode at 1061 cm^{-1}.

STRUCTURE REFINEMENT

Structural refinement of $BaNiO_2$ using the Rietveld method has been carried out using powder neutron diffraction data. The atomic positions used as the starting point for the refinement were the metal and oxide coordinates reported for $BaCuO_2$ by Aranda and Attfield from a combined powder X-ray and powder neutron diffraction study, but with nickel on the copper sites. Initial iterations in the refinement included background parameters, the histogram scale factor, peak shapes, and lattice parameter. Two impurity phases were identified as contributing weak reflections to the neutron diffraction pattern, namely nickel metal and nickel oxide, and these were added to the refinement and modeled alongside $BaNiO_2$. The atomic coordinates of all three barium positions and the first three nickel positions of $BaNiO_2$ were allowed to vary and refined satisfactorily. The refinement of the oxygen coordinates involved in the $Ni_{18}O_{24}$ cages and the Ni_6O_{12} rings (O(1), O(2), and O(3)) could also be achieved successfully, leading to satisfactory bond lengths and angles. However, the fit factors obtained at this stage were relatively high with χ^2 above six. Carbonate groups were then added to the refined model, giving four possible orientations located between two different Ni_6O_{12} rings, in agreement with the structure of $BaCuO_2$. The introduction of a disordered carbonate anion, as used by Aranda and Attfield, improved the fit considerably and led to a convergent refinement with a χ^2 value of 4.465 and an R_{wp} of 5.49%. However, refinement of the Ni(4) position, $(0, 0, z)$ with $z \approx 0.43$, produced an unstable refinement with large temperature factors obtained for this atom. A new structural model was required to improve the profile fit and provide information on this disordered region of the unit cell; this region is located approximately half way along the unit cell axes between two $Ni_{18}O_{24}$ cages. A difference Fourier map of this area was calculated, using the 300 reflections in the observed data range, and is shown in Fig. 2. The four regions of high scattering density located around the center of the map are broad in comparison with the other features and separated by distances which did not correlate with any known species likely to be present. This indicated that the occupation of this section of the structure is not restricted to a single species but requires the development of a more complex model. The separation of the centers of the Fourier peaks, approximately 1.7 Å, was similar to the refined Cu–O distance in $BaCuO_2$ and may represent a hybrid of bond lengths. This distance lies approximately midway between a typical C–O bond length (1.3 Å) and a Ni–O bond length (1.95 Å). The structural model envisaged for this section of the structure is illustrated in Fig. 3. This representation indicates a partial occupation of this site by trigonal planar CO_3, isolated NiO_4 square planes, and vacancies, creating an average which complies with the calculated difference Fourier map. The diffuseness of the Fourier peaks derives from the close vicinity of the CO_3 and NiO_4 groups; any attempts to model scattering from this area of the structure using a

TABLE 2
Vibrational Spectroscopy Data and Assignment of $BaNiO_2$

Infrared wavelength/cm^{-1}	Vibrational assignment in C_{2v} symmetry
1410–1380	$\nu_3(A_1 + B_1)$
1054.4	$\nu_1(A_1)$
855.9	$\nu_2(B_1)$
698.8, 684.6	$\nu_4(A_1 + B_2)$

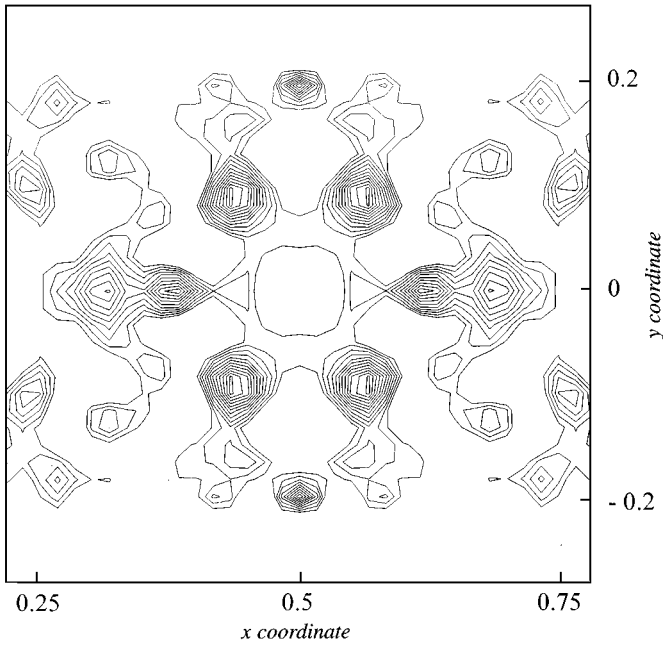

FIG. 2. A difference Fourier map of $BaNiO_2$ showing the disordered region of the structure ($z = 0$) located between two $Ni_{18}O_{24}$ clusters.

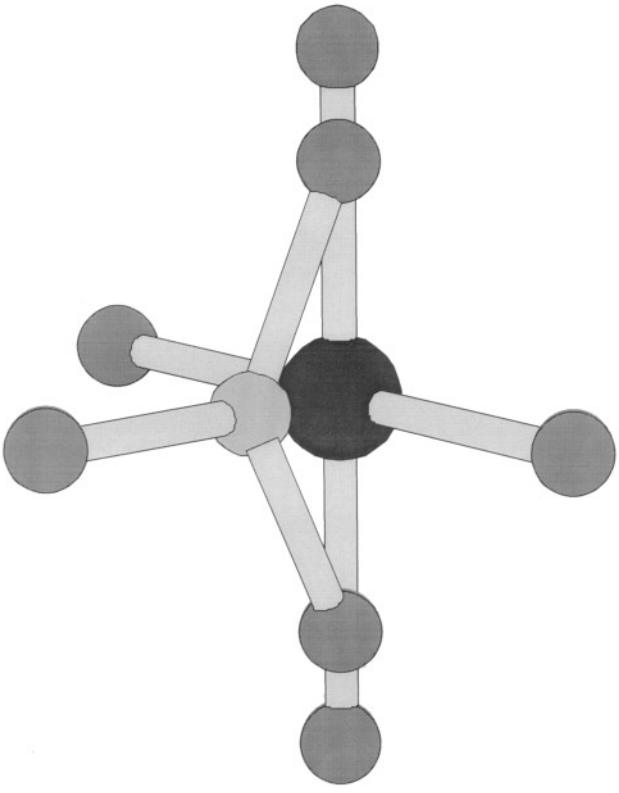

FIG. 3. Combination of trigonal planar carbonate and square planar NiO_4^{6-} groups used to model the disordered region of the structure. The refined geometries and relative positions obtained are shown.

single moiety would give rise to averaged, intermediate bond lengths, for example, the 1.69 Å Cu–O distance found by Aranda and Attfield (11). Unfortunately, modeling this disorder also leads to difficulties in the Rietveld refinement, making absolute determination of this region very difficult. A constrained refinement using a model with partial occupancy at the site of CO_3 and NiO_4 was undertaken. Occupancy of the site by these species was maintained at a level to give a nickel oxidation state of 2+, in agreement with that determined by Gottschall and Schöllhorn (22) producing a refined stoichiometry for the material of $Ba_{88}Ni_{87}O_{156}(CO_3)_{19}$. The application of soft constraints was necessary to maintain sensible values for several bond distances (Ni(4)–O(4) 1.836 Å, $\sigma = 0.002$, C(1)–O(8) 1.250 Å, $\sigma = 0.003$, and C(1)–O(5) 1.250 Å, $\sigma = 0.003$). Also, the Ni(4) and O(4) z positions were tied to ensure NiO_4 square planes.

The final model (space group $Im\bar{3}m$, $a = 18.0532(1)$ Å is given in Table 3, and gives a good fit ($\chi^2 = 3.15$, $R_{wp} = 4.62\%$) to the powder neutron diffraction profile (Fig. 4), and produced reasonable bond lengths (Table 4). The final refined structure is illustrated in Fig. 5.

Rietveld refinement of $BaPdO_2$ was initially undertaken using powder X-ray data employing the starting coordinates reported for $BaCuO_2$, but with palladium on the copper sites. Well defined barium and palladium positions were obtained although oxygen positions were unstable and therefore no useful information could be derived about the

TABLE 3
Atomic Parameters for $Ba_{88}Ni_{87}O_{156}(CO_3)_{19}$

Atom	Position	x	y	z	B_{eq}	Occupancy
Ba(1)	48j	0	0.15311(14)	0.30972(12)	1.43(13)	1
Ba(2)	24g	0	0.36565(10)	0.36565(10)	0.85(15)	1
Ba(3)	16f	0.17845(12)	0.17845(12)	0.17845(12)	0.80(10)	1
Ni(1)	48i	0.15141(4)	0.34859(4)	$\frac{1}{4}$	0.38(5)	1
Ni(2)	24g	0	0.12757(10)	0.12757(10)	5.67(12)	1
Ni(3)	12e	0	0	0.19720(14)	1.54(11)	1
Ni(4)	12e	0	0	0.4445(4)	3.8(2)	0.245[a]
O(1)	48k	0.07276(9)	0.07276(9)	0.18960(15)	2.69(12)	1
O(2)	48k	0.14794(7)	0.14794(7)	0.33881(11)	0.55(9)	1
O(3)	48k	0.27058(8)	0.27058(8)	0.08391(9)	0.15(8)	1
C(1)	12e	0	0	0.4055(5)	3.8(2)	0.599[a]
O(4)	48j	0	0.10134(10)	0.4445(4)	1.8(2)	0.245[a]
O(5)	12e	0.3413(6)	0	0	6.0(3)	0.599[a]
O(6)	48j	0.2148(3)	0	0.4436(3)	5.2(2)	$\frac{1}{2}$
O(7)	48i	$\frac{1}{4}$	0.0638(3)	0.4362(3)	1.1(4)	$\frac{1}{4}$
C(2)	12d	$\frac{1}{4}$	0	$\frac{1}{2}$	0[b]	1
O(8)	48j	0	0.0650(3)	0.4284(5)	2.6(2)	0.299[a]

Note. $\chi^2 = 3.15$, $R_{wp} = 4.62\%$.
[a] These parameters led to instabilities in the refinement when varied alongside atomic coordinates and temperature factors.
[b] Temperature factor refines to less than zero.

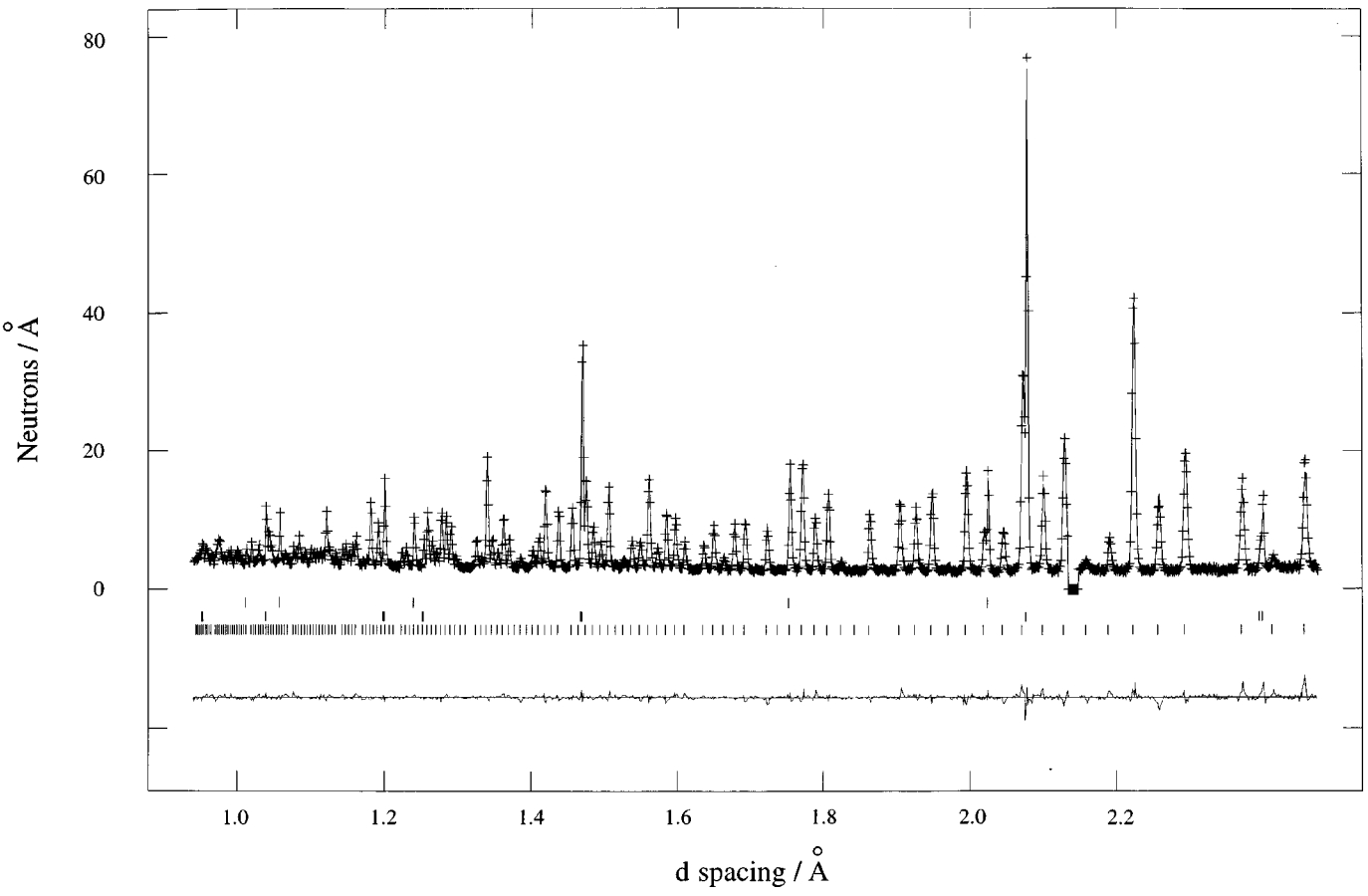

FIG. 4. Final fit obtained to the powder neutron diffraction profile of $BaNiO_2$ in the range 0.95–2.5 Å. Crosses indicate observed data points, the upper continuous line shows the calculated profile, and the lower continuous line is the difference. Tick marks show reflection positions $BaNiO_2$ (lower), NiO (center), and Ni (upper).

TABLE 4
Refined Bond Lengths for $BaNiO_2$

Bond	Length/Å	No.	Bond	Length/Å	No.
Ba(1)–O(1)	2.920(3)	×2	Ba(2)–O(8)	3.017(4)	×1.196
Ba(1)–O(2)	2.7278(14)	×2	Ba(3)–O(1)	2.707(3)	×3
Ba(1)–O(3)	2.6999(22)	×2	Ba(3)–O(2)	2.998(2)	×3
Ba(1)–O(4)	2.612(7)	×0.245	Ba(3)–O(3)	2.905(2)	×3
Ba(1)–O(5)	2.824(4)	×0.599	Ni(1)–O(2)	1.8519(14)	×2
Ba(1)–O(6)	2.655(7)	×0.5	Ni(1)–O(3)	1.8988(14)	×2
Ba(1)–O(7)	3.098(3)	×0.5	Ni(1)–O(7)	2.237(7)	×0.25
Ba(1)–O(8)	2.667(8)	×0.299	Ni(2)–O(1)	1.9893(14)	×4
Ba(2)–O(2)	2.9294(19)	×2	Ni(3)–O(1)	1.862(2)	×4
Ba(2)–O(3)	2.861(2)	×2	Ni(4)–O(4)	1.8292(17)	×4
Ba(2)–O(4)	2.688(3)	×0.980	C(1)–O(5)	1.160(12)	×1
Ba(2)–O(6)	3.064(6)	×1	C(1)–O(8)	1.244(5)	×2
Ba(2)–O(6)	3.005(3)	×2	C(2)–O(6)	1.200(6)	×2
Ba(2)–O(7)	2.7030(6)	×1	C(2)–O(7)	1.629(7)	×1
Carbonate bond angles					
O(5)–C(1)–O(8)	109.4(5)°		O(7)–C(2)–O(6)	126.9(1)°	
O(8)–C(1)–O(8)	141.3(10)°		O(6)–C(2)–O(6)	106.3(2)°	

Note. All bond multiplicities take into account site occupancies.

partially occupied disordered region. In order to delineate this region of the structure, powder neutron diffraction data were required.

Refinement of the powder neutron data, using the starting model derived from the powder X-ray refinement, was subsequently undertaken. The initial refinement iterations included background parameters, the histogram scale factor, peak shape parameters, and the lattice parameter. Palladium metal was identified as an impurity contributing weakly to the profile and its structure included in the refinement. The heavy atoms present within the structure were then refined (with the exception of Pd(4) on $(0, 0, z)$ $z \approx 0.43$) and showed little variation from the positions determined using powder X-ray data. The refinement of the oxygen coordinates involved in the $Pd_{18}O_{24}$ cages and the Pd_6O_{12} rings (O(1), O(2), and O(3)) could be achieved successfully, as with the nickelate, and led to satisfactory bond lengths and angles. Carbonate was incorporated into the refinement model as with the nickelate system.

In order to fit the data application of the model determined for the nickelate system was required. The site near

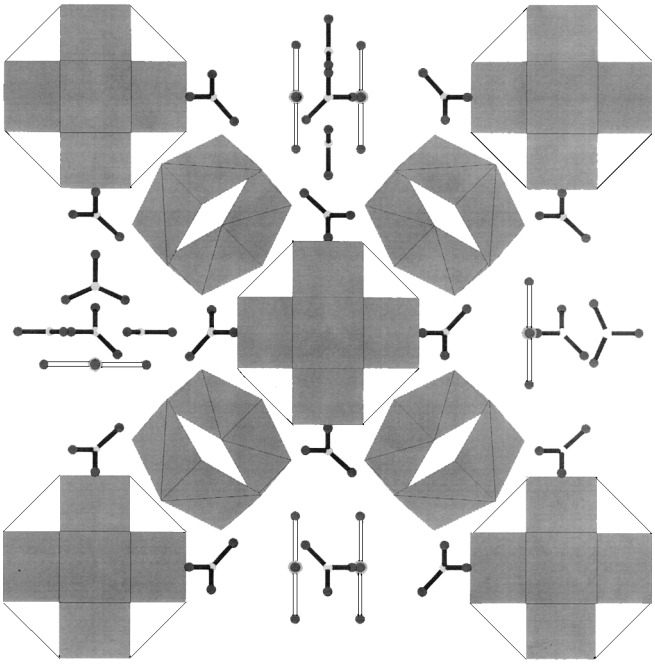

FIG. 5. The structure of $BaNiO_2$, containing $Ni_{18}O_{24}$ cages, Ni_6O_{12} rings, discrete NiO_4 square planes, and trigonal planar CO_3 groups. Barium ions have been omitted for clarity.

(0, 0, 0.4) was again modeled using a combination of carbonate and PdO_4 with partial occupancy by both species. Occupancies of both the PdO_4 and CO_3 groups were refined to maintain an oxidation state for palladium of 2+ and leading to the refined stoichiometry $Ba_{11}Pd_{11}O_{20}(CO_3)_2$. Constraints were again used in the refinement to maintain charge balance and restrain several bond lengths (C(1)–O(5) 1.270 Å, $\sigma = 0.003$, C(1)–O(6) 1.270 Å, $\sigma = 0.003$). Discrete PdO_4 square planes were maintained within the disordered region by tying together the z coordinates of Pd(4) and O(8). This model improved the fit considerably giving the final fit parameters $\chi^2 = 5.576$, $R_{wp} = 5.90\%$ (Fig. 6). The final model of the structure (space group $Im\bar{3}m$, $a = 18.42937(3)$ Å) is detailed in Table 5. The refined bond lengths within the structure are shown in Table 6.

DISCUSSION

A new complex palladate analog of a known cuprate structure has been synthesized but for the first time a material containing carbonate ions has been isolated. The structure of the previously described barium nickelate carbonate has been confirmed as a member of this family. A surprising

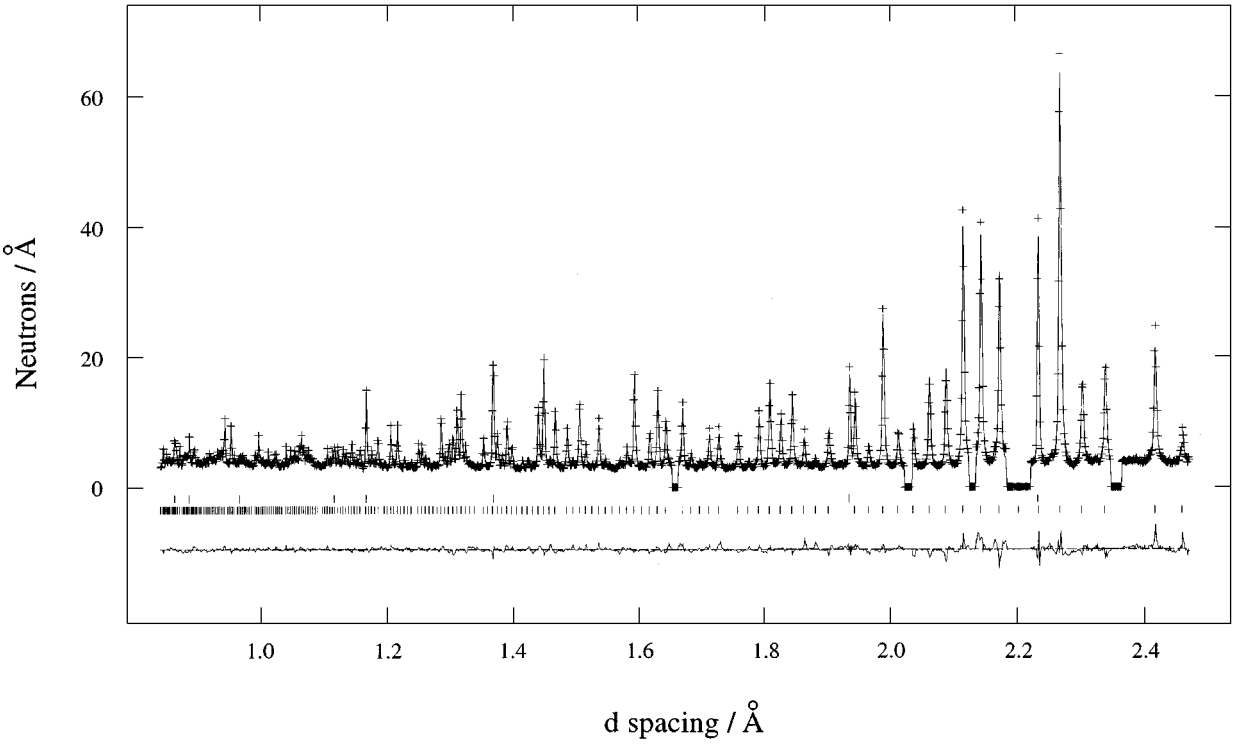

FIG. 6. Final fit obtained to the powder neutron diffraction profile of $BaPdO_2$ in the range 0.85–2.45 Å. Crosses indicate observed data points, the upper continuous line shows the calculated profile, and the lower continuous line is the difference. Tick marks show the reflection positions $BaPdO_2$ (lower) and Pd (upper).

TABLE 5
Atomic Positions for $Ba_{11}Pd_{11}O_{20}(CO_3)_2$

Atom	Position	x	y	z	B_{eq}	Occupancy
Ba(1)	48*j*	0	0.15290(14)	0.30798(13)	1.11(13)	1
Ba(2)	24*g*	0	0.36929(13)	0.36929(13)	1.28(17)	1
Ba(3)	16*f*	0.17911(13)	0.17911(13)	0.17911(13)	0.71(10)	1
Pd(1)	48*i*	0.14558(7)	0.35482(7)	$\frac{1}{4}$	0.48(9)	1
Pd(2)	24*g*	0	0.13520(14)	0.13520(14)	3.47(18)	1
Pd(3)	12*e*	0	0	0.20323(25)	2.65(25)	1
Pd(4)	12*e*	0	0	0.4303(5)	0.56(24)	0.3333[a]
O(1)	48*k*	0.07624(9)	0.07624(9)	0.19539(12)	1.70(9)	1
O(2)	48*k*	0.14094(7)	0.14094(7)	0.34579(11)	0.84(9)	1
O(3)	48*k*	0.27158(8)	0.27158(8)	0.07763(11)	0.76(8)	1
O(4)	48*i*	$\frac{1}{4}$	0.04783(26)	0.45217(26)	9.6(5)	$\frac{1}{4}$
C(1)	12*e*	0	0	0.4031(8)	0.56(24)	0.3333[a]
O(5)	48*j*	0	0.0635(5)	0.4316(8)	2.97(23)	0.1667[a]
O(6)	12*e*	0	0	0.3351(8)	8.7(8)	0.3333[a]
O(7)	48*j*	0.20274(34)	0	0.44834(19)	2.5(3)	$\frac{1}{2}$
C(2)	12*d*	$\frac{1}{4}$	0	$\frac{1}{2}$	1.4(2)	1
O(8)	48*j*	0	0.10949(7)	0.4303(5)	6.48(23)	0.3333[a]

Note. $\chi^2 = 5.576$, $R_{wp} = 5.90\%$.
[a] These parameters led to instabilities in the refinement when varied alongside atomic coordinates and temperature factors.

feature of this structural chemistry is the stability of the large unit cell with its complex structural motifs of $M_{18}O_{24}$ cages and M_6O_{12} rings built from edge sharing MO_4 square planes. The high formal charge on a $[M^{2+}O_4]^{6-}$ unit means that unless the counter cations present in a structure are themselves highly charged, e.g., bismuth in Bi_2PdO_4, then the square planar units do not occur as discrete species. More commonly these units form one-dimensional chains through edge sharing, e.g., Li_2PdO_2 (23) but other structures such as $PbPdO_2$ (24), in which corner sharing square planes form alternating chains along two axis, are also found. The M_6O_{12} six rings found in $BaPdO_2$ also occur in $CaBa_2Pd_3O_6$ (25), however the $Pd_{18}O_{24}$ cages have not been described previously. These elements of the structure are well defined in the refinements allowing oxidation states to be calculated using the bond valence parameters of Brown and Altermatt (26) for the various palladium/nickel sites. This approach has been employed here and the results are summarized in Tables 7 and 8. For structures with rigid structural elements, such as the square planar units forming the cages and rings, these calculations can often show significant deviations from the true oxidation states. The results in Tables 7 and 8 show reasonable values for all ions though in both the palladate and nickelate the values associated with the cation on the 24*g* site $(0, x, x)$ are low. This atom also has a relatively high temperature factor for both structures. These factors may indicate that this atom is in fact

TABLE 6
Refined Bond Lengths for $BaPdO_2$

Bond	Length/Å	No.	Bond	Length/Å	No.
Ba(1)–O(1)	2.8767(27)	×2	Ba(3)–O(1)	2.698(4)	×3
Ba(1)–O(2)	2.6982(14)	×2	Ba(3)–O(2)	3.2289(25)	×3
Ba(1)–O(3)	2.6983(22)	×2	Ba(3)–O(3)	3.0506(22)	×3
Ba(1)–O(5)	2.812(17)	×0.1667	Pd(1)–O(2)	2.0183(13)	×2
Ba(1)–O(6)	2.8619(34)	×0.333	Pd(1)–O(3)	2.0152(16)	×2
Ba(1)–O(7)	2.745(4)	×0.5	Pd(2)–O(1)	2.0942(11)	×4
Ba(1)–O(8)	2.392(9)	×0.333	Pd(3)–O(1)	1.9922(24)	×4
Ba(2)–O(2)	2.8545(19)	×2	Pd(4)–O(8)	2.0178(12)	×4
Ba(2)–O(3)	2.921(4)	×2	C(1)–O(5)	1.283(4)	×2
Ba(2)–O(4)	2.8184(12)	×1	C(1)–O(6)	1.253(7)	×1
Ba(2)–O(5)	2.988(6)	×0.666	C(2)–O(7)	1.247(7)	×2
Ba(2)–O(7)	2.9106(35)	×2	C(2)–O(4)	1.290(5)	×1
Ba(2)–O(8)	2.758(5)	×1.333			
Carbonate bond angles					
O(4)–C(2)–O(7)	121.4(1)°		O(6)–C(1)–O(5)	114.2(1)°	
O(7)–C(2)–O(7)	117.1(2)°		O(5)–C(1)–O(5)	131.6(2)°	

Note. All bond multiplicities take into account site occupancies.

TABLE 7
Bond Valence Calculations for $BaNiO_2$

Atom	Calculated oxidation state	Atom	Calculated oxidation state
Ba(1)	2.20	Ni(2)	1.62
Ba(2)	2.00	Ni(3)	2.28
Ba(3)	1.96	Ni(4)	2.49
Ni(1)	2.26		

TABLE 8
Bond Valence Calculations for $BaPdO_2$

Atom	Calculated oxidation state	Atom	Calculated oxidation state
Ba(1)	2.22	Pd(2)	1.73
Ba(2)	1.86	Pd(3)	2.29
Ba(3)	1.60	Pd(4)	2.13
Pd(1)	2.14		

disordered off the special site or that it has a partial occupancy, though no stable displacement could be refined.

The $BaCuO_2$ structure has proved unsatisfactory for modeling the disordered region, and the refinement statistics have been improved using a random distribution of nickelate/palladate, carbonate, and vacancies about the site near (0, 0, 0.4). However, despite the quality of the diffraction data the true nature of the species occupying this region cannot be unambiguously defined. The model used explains the previously unacceptable bond lengths but because of the simultaneous occupation of part of the structure by more than one species constraints are necessary in the refinement. In the palladate the presence of a random distribution of PdO_4 square planes and carbonate probably leads to a distribution in the positions of the associated barium positions (Ba(1)). This has not been accounted for in the refinement and leads to a somewhat short Ba(1)–O(8) bond length of 2.392(9) Å.

ACKNOWLEDGMENTS

We thank the EPSRC for a studentship for RJC, a grant in support of this work, and the provision of neutron beam facilities at the Rutherford-Appleton Laboratory. We also thank A. M. Healey and E. Llewellyn for help in collecting the Raman spectra.

REFERENCES

1. D. M. Ogborne, M. T. Weller, and P. C. Lanchester, *Physica C* **200,** 207 (1992).
2. R. L. Needs and M. T. Weller, *J. Chem. Soc. Chem. Commun.* 353 (1995).
3. P. R. Slater, C. Greaves, M. Slaski, and C. M. Muirhead, *Physica C* **205,** 193 (1993).
4. S. M. Emelyanov and G. A. Gegazina, *Inorg. Mater.* **20(10),** 1744 (1984).
5. A. Maignan, M. Hervieu, C. Michel, and B. Raveau, *Physica C* **208,** 116 (1993).
6. G. Baud, J. P. Besse, M. Capestan, G. Sueur, and R. Chevalier, *Ann. Chim.* (*Paris*) **5,** 573 (1980).
7. T. Sakurai, T. Nishino, and Y. Kyokaishi, *J. Ceram. Assoc. Jpn.* **91,** 126 (1983).
8. R. L. Meng, L. Beauvais, X. N. Zhang, Z. J. Huang, Y. Y. Sun, Y. Y. Xue, and C. W. Chu, *Physica C* **216,** 21 (1993).
9. R. Kipka and Hk. Müller-Buschbaum, *Z. Naturforsch. B* **32,** 121 (1977).
10. D. R. Lines and M. T. Weller, *J. Chem. Soc. Chem. Commun.* 484 (1989).
11. M. A. G. Aranda and J. P. Attfield, *Angew. Chem. Int. Ed. Engl.* **10,** 32 (1993).
12. N. Guskos, V. Likodimus, C. A. Londos, V. Psycharis, C. Mitros, A. Koufoudakis, H. Gamari-Seale, W. Windsch, and H. Metz, *J. Solid State Chem.* **119,** 50 (1995).
13. D. R. Lines, M. T. Weller, D. B. Currie, and D. M. Ogborne, *Mater. Res. Bull.* **26(4),** 323 (1991).
14. D. M. Ogborne and M. T. Weller, *Physica C* **223,** 283 (1994).
15. M. T. Weller and D. R. Lines, *J. Solid State Chem.* **82,** 21 (1989).
16. H. D. Wasel-Nielen and R. Hoppe, *Z. Anorg. Allg. Chem.* **375(3),** 209 (1970).
17. Hk. Müller-Buschbaum and R. Arpe, *Z. Anorg. Allg. Chem.* **426,** 1 (1976).
18. C. Chaillout, S. W. Cheong, Z. Fisk, M. S. Lehmann, M. Marezio, B. Morosin, and J. E. Schirber, *Physica C* **158,** 183 (1989).
19. D. J. Buttrey and J. M. Honig, *J. Solid State Chem.* **72,** 38 (1988).
20. A. K. Ganguli and M. A. Subramanian, *J. Solid State Chem.* **93,** 250 (1991).
21. C. S. Knee and M. T. Weller, *J. Mater. Chem.* **6,** 1449 (1996).
22. R. Gottschall and R. Schöllhorn, *Solid State Ionics* **59,** 93 (1993).
23. J. P. Attfield and G. Ferey, *J. Solid State Chem.* **80,** 286 (1989).
24. H. Meyer and Hk. Müller-Buschbaum, *Z. Anorg. Chem.* **442,** 26 (1978).
25. P. Sonne and Hk. Müller-Buschbaum, *Z. Anorg. Chem.* **619,** 1004 (1993).
26. I. D. Brown and D. Altermatt, *Acta. Crystallogr. Sect. B* **41,** 244 (1985).